Bull. Astr. Soc. India (2011) **39**, 145–161

The formation and evolution of massive black hole seeds in the early Universe

Priyamvada Natarajan,[1,2,3]*

[1]*Department of Astronomy, Yale University, 260 Whitney Avenue, New Haven, CT 06511*
[1]*Department of Physics, Yale University, P.O. Box New Haven, CT 06520*
[3]*Institute for Theory and Computation, Harvard University, 60 Garden Street, Cambridge MA 02138*

Received 2011 February 27; accepted 2011 March 24

Abstract. Tracking the evolution of high redshift seed black hole masses to late times, we examine the observable signatures today. These massive initial black hole seeds form at extremely high redshifts from the direct collapse of pre-galactic gas discs. Populating dark matter halos with seeds formed in this fashion, we follow the mass assembly history of these black holes to the present time using a Monte-Carlo merger tree approach. Utilizing this formalism, we predict the black hole mass function at high redshifts and at the present time; the integrated mass density of black holes in the Universe; the luminosity function of accreting black holes as a function of redshift and the scatter in observed, local $M_{\rm bh} - \sigma$ relation. Comparing the predictions of the 'light' seed model with these massive seeds we find that significant differences appear predominantly at the low mass end of the present day black hole mass function. However, all our models predict that low surface brightness, bulge-less galaxies with large discs are least likely to be sites for the formation of massive seed black holes at high redshifts. The efficiency of seed formation at high redshifts has a direct influence on the black hole occupation fraction in galaxies at $z = 0$. This effect is more pronounced for low mass galaxies. This is the key discriminant between the models studied here and the Population III remnant 'light' seed model. We find that there exists a population of low mass galaxies that do not host nuclear black holes. Our prediction of the shape of the $M_{\rm bh} - \sigma$ relation at the low mass end and increased scatter has recently been corroborated by observations.

Keywords : black holes – galaxies: evolution – galaxies: high redshift

*e-mail:priyamvada.natarajan@yale.edu

1. Introduction

Demography of local galaxies suggests that most galaxies harbour quiescent super-massive black holes (SMBHs) in their nuclei at the present time and that the mass of the hosted SMBH is correlated with properties of the host bulge. In fact, observational evidence points to the existence of a strong correlation between the mass of the central SMBH and the velocity dispersion of the host spheroid (Tremaine et al. 2002; Ferrarese & Merritt 2000, Gebhardt et al. 2003; Marconi & Hunt 2003; Häring & Rix 2004; Gültekin et al. 2009) and possibly the host halo (Ferrarese 2002) in nearby galaxies. These correlations are strongly suggestive of co-eval growth of the SMBH and the stellar component, likely via regulation of the gas supply in galactic nuclei from the earliest times (Haehnelt, Natarajan, Rees 1998; Silk & Rees 1999; Kauffmann & Haehnelt 2000; Fabian 2002; King 2003; Thompson, Quataert & Murray 2005; Natarajan & Treister 2009).

2. Links between massive SMBH seeds, halo mass and spin

Optically bright quasars powered by accretion onto black holes are now detected out to redshifts of $z > 6$ when the Universe was barely 7% of its current age (Fan et al. 2004; 2006). The luminosities of these high redshift quasars imply black hole masses $M_{\rm BH} > 10^9\,M_\odot$. Models that describe the growth and accretion history of supermassive black holes typically use as initial seeds the remnants derived from Pop-III stars (e.g. Haiman & Loeb 1998; Haehnelt, Natarajan & Rees 1998). Assembling these large black hole masses by this early epoch starting from remnants of the first generation of metal free stars has been a challenge for models. Some suggestions to accomplish rapid growth invoke super-Eddington accretion rates for brief periods of time (Volonteri & Rees 2005). Alternatively, it has been suggested that the formation of more massive seeds ab-initio through direct collapse of self-gravitating pre-galactic disks might offer a new channel as proposed by Lodato & Natarajan 2006 [LN06]. This scenario alleviates the problem of building up supermassive black hole masses to the required values by $z = 6$.

We focus on the main features of massive seed models in this review. Most aspects of the evolution and assembly history of this scenario have been explored in detail in Volonteri & Natarajan (2009) and Volonteri, Lodato & Natarajan (2008). In these models, at early times the properties of the assembling SMBH seeds are more tightly coupled to properties of the dark matter halo as their growth is driven by the merger history of halos. However, at later times, when the merger rates are low, the final mass of the SMBH is likely to be more tightly coupled to the small scale local baryonic distribution. The relevant host dark matter halo property at high redshifts in this picture is the spin.

In a physically motivated model for the formation of heavy SMBH seeds (in contrast to the lower mass remnant seeds from Population III stars) as described in LN06, there is a limited range of halo spins and halo masses that are viable sites for the formation of seeds. In this picture, massive seeds with $M \approx 10^5 - 10^6 M_\odot$ can form at high redshift ($z > 15$), when the intergalactic medium has not been significantly enriched by metals (Koushiappas, Bullock & Dekel 2004; Begelman, Volonteri & Rees 2006; LN06; Lodato & Natarajan 2007). As derived in LN06, the

development of non-axisymmetric spiral structures drives mass infall and accumulation in a pre-galactic disc with primordial composition. The mass accumulated in the center of the halo (which provides an upper limit to the SMBH seed mass) is given by:

$$M_{\rm BH} = m_{\rm d} M_{\rm halo} \left[1 - \sqrt{\frac{8\lambda}{m_{\rm d} Q_{\rm c}} \left(\frac{j_{\rm d}}{m_{\rm d}} \right) \left(\frac{T_{\rm gas}}{T_{\rm vir}} \right)^{1/2}} \right] \tag{1}$$

for

$$\lambda < \lambda_{\rm max} = m_{\rm d} Q_{\rm c} / 8 (m_{\rm d} / j_{\rm d}) (T_{\rm vir} / T_{\rm gas})^{1/2} \tag{2}$$

and $M_{\rm BH} = 0$ otherwise. Here $\lambda_{\rm max}$ is the maximum halo spin parameter for which the disc is gravitationally unstable, m_d is the gas fraction that participates in the infall and $Q_{\rm c}$ is the Toomre parameter. The efficiency of SMBH formation is strongly dependent on the Toomre parameter $Q_{\rm c}$, which sets the frequency of formation, and consequently the number density of SMBH seeds. The efficiency of the seed assembly process ceases at large halo masses, where the disc undergoes fragmentation instead. This occurs when the virial temperature exceeds a critical value $T_{\rm max}$, given by:

$$\frac{T_{\rm max}}{T_{\rm gas}} = \left(\frac{4\alpha_{\rm c}}{m_{\rm d}} \frac{1}{1 + M_{\rm BH} / m_{\rm d} M_{\rm halo}} \right)^{2/3}, \tag{3}$$

where $\alpha_{\rm c} \approx 0.06$ is a dimensionless parameter measuring the critical gravitational torque above which the disc fragments. The remaining relevant parameters are assumed to have typical values: $m_{\rm d} = j_{\rm d} = 0.05$, $\alpha_{\rm c} = 0.06$ for the $Q_{\rm c} = 2$ case. The gas has a temperature $T_{\rm gas} = 5000$K.

To summarize, every dark matter halo is characterized by its mass M (or virial temperature $T_{\rm vir}$) and by its spin parameter λ. If $\lambda < \lambda_{\rm max}$ (see equation 2) and $T_{\rm vir} < T_{\rm max}$ (equation 3), then a seed SMBH forms in the centre. Hence SMBHs form (i) only in halos within a given range of virial temperatures, and hence, halo masses, and (ii) only within a narrow range of spin parameters, as shown in Figure 1. High values of the spin parameter, leading most likely to disk-dominated galaxies, are strongly disfavored as seed formation sites in this model, and in models that rely on global dynamical instabilities (Volonteri & Begelman 2010).

3. The evolution of seed black holes

We follow the evolution of the MBH population resulting from the seed formation process delineated above in a ΛCDM Universe. Our approach is similar to the one described in Volonteri, Haardt & Madau (2003). We simulate the merger history of present-day halos with masses in the range $10^{11} < M < 10^{15}\, M_{\odot}$ starting from $z = 20$, via a Monte Carlo algorithm based on the extended Press-Schechter formalism. Every halo entering the merger tree is assigned a spin parameter drawn from the lognormal $P(\lambda)$ distribution of simulated LCDM halos. Recent work on the fate of halo spins during mergers in cosmological simulations has led to conflicting results: Vitvitska et al. (2002) suggest that the spin parameter of a halo increases after a major merger, and the angular momentum decreases after a long series of minor mergers; D'Onghia & Navarro

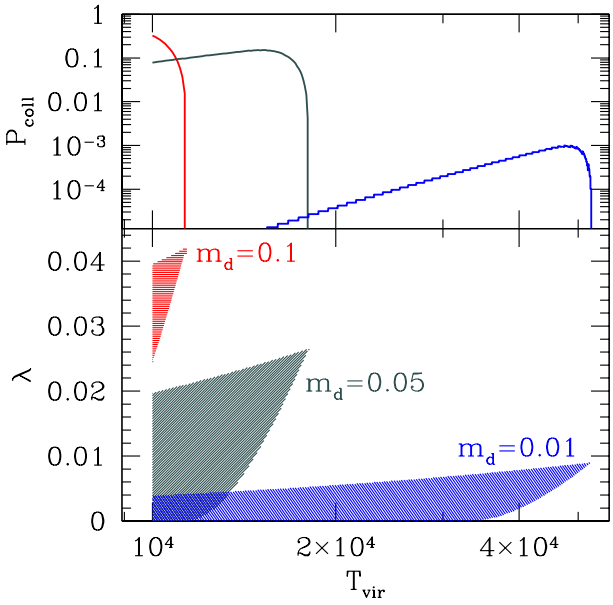

Figure 1. Parameter space (virial temperature, spin parameter) for SMBH formation. Halos with $T_{vir} > 10^4$ K at $z = 15$ are picked to participate in the infall ($m_{\rm d}$). The shaded areas in the bottom panel show the range of virial temperatures and spin parameters where discs are Toomre unstable and the joint conditions, $\lambda < \lambda_{\rm max}$ (equation 2) and $T_{\rm vir} < T_{\rm max}$ (equation 3, showing the minimum spin parameter, $\lambda_{\rm min}$ value below which the disc is globally prone to fragmentation) are fulfilled. The top panel shows the probability of SMBH formation and is obtained by integrating the lognormal distribution of spin parameters between $\lambda_{\rm min}$ and $\lambda_{\rm max}$.

(2007) find instead no significant correlation between spin and merger history. Given the unsettled nature of this matter, we simply assume that the spin parameter of a halo is not modified by its merger history.

When a halo enters the merger tree we assign seed MBHs by determining if the halo meets all the requirements described in Section 2 for the formation of a central mass concentration. As we do not self-consistently trace the metal enrichment of the intergalactic medium, we consider here a sharp transition threshold, and assume that the MBH formation scenario suggested by Lodato & Natarajan ceases at $z \approx 15$ (see also Sesana 2007; Volonteri 2007). At $z > 15$, therefore, whenever a new halo appears in the merger tree (because its mass is larger than the mass resolution), or a pre-existing halo modifies its mass by a merger, we evaluate if the gaseous component meets the conditions for efficient transport of angular momentum to create a large inflow of gas which can either form a MBH seed, or feed one if already present.

The efficiency of MBH formation is strongly dependent on a critical value of the Toomre parameter $Q_{\rm c}$, which sets the frequency of formation, and consequently the number density of

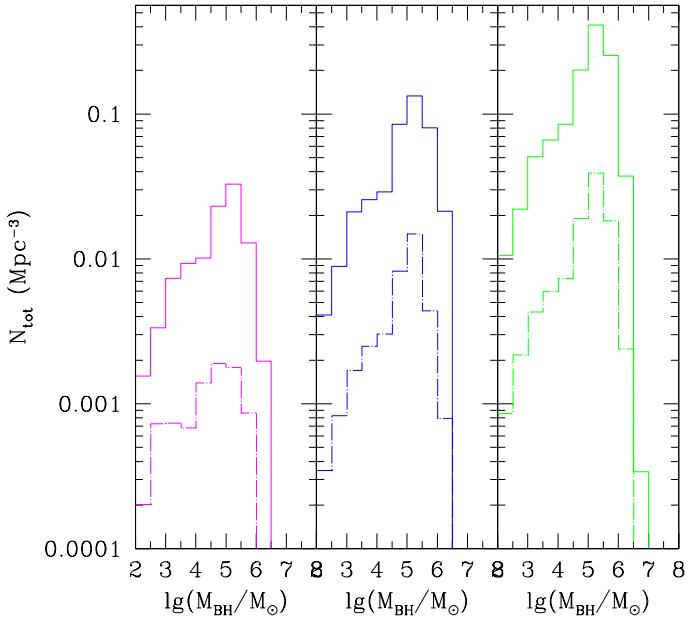

Figure 2. Mass function of MBH seeds in the three Q-models that differ in seed formation efficiency. Left panel: $Q_c = 1.5$ (the least efficient model A), middle panel: $Q_c = 2$ (intermediate efficiency model B), right panel: $Q_c = 3$ (highly efficient model C). Seeds form at $z > 15$ and this channel ceases at $z = 15$. The solid histograms show the total mass function of seeds formed by $z = 15$, while the dashed histograms refer to seeds formed at a specific redshift, $z = 18$.

MBH seeds. We investigate the influence of this parameter in the determination of the global evolution of the MBH population. Figure 2 shows the number density of seeds formed in three different models with varying efficiency, with $Q_c = 1.5$ (low efficiency model A), $Q_c = 2$ (intermediate efficiency model B), and $Q_c = 3$ (high efficiency model C). The solid histograms show the total mass function of seeds formed by $z = 15$ when this formation channel ceases, while the dashed histograms refer to seeds formed in a specific redshift slice at $z = 18$. The number of seeds changes by about one order of magnitude from the least efficient to the most efficient model, consistent with the probabilities shown in Figure 1.

We assume that, after seed formation ceases, the $z < 15$ population of MBHs evolves according to a "merger driven scenario", as described in Volonteri (2006). We assume that during major mergers MBHs accrete gas mass that scales with the fifth power of the circular velocity (or equivalently the velocity dispersion σ_c) of the host halo (Ferrarese 2002). We thus set the final mass of the MBH at the end of the accretion episode to 90% of the mass predicted by the $M_{\rm BH} - \sigma_c$ correlation, assuming that the scaling does not evolve with redshift. Major mergers are defined as mergers between two dark matter halos with mass ratio between 1 and 10. BH mergers contribute to the mass addition of the remaining 10%.

We briefly outline the merger scenario calculation here. The merger rate of halos can be estimated using equation 1 of Fakhouri, Ma & Boylan-Kolchin (2010), where a simple fitting formula is derived from large LCDM simulations. The merger rate per unit redshift and mass ratio (ξ) at fixed halo mass is given by:

$$\frac{dN_m}{d\xi dz}(M_h) = A\left(\frac{M_h}{10^{12}M_0}\right)^{\alpha} \xi^{\beta} \exp\left[\left(\frac{\xi}{\tilde{\xi}}\right)^{\gamma}\right](1+z)^{\eta}. \quad (4)$$

with A = 0.0104, $\alpha = 0.133$, $\beta = -1.995$, $\gamma = 0.263$, $\eta = 0.0993$ and $\tilde{\xi} = 9.72 \times 10^{-3}$. We can integrate the merger rate between $z = 0$ and say, $z = 3$, for major mergers. This gives the number of major mergers a halo of a given mass experiences between $z = 0$ and $z = 3$. Halo mass can be translated into virial circular velocity:

$$V_{\rm c} = 142{\rm km/s}\left[\frac{M_{\rm h}}{10^{12}\ M_{\odot}}\right]^{1/3}\left[\frac{\Omega_m}{\Omega_m^z}\ \frac{\Delta_{\rm c}}{18\pi^2}\right]^{1/6}(1+z)^{1/2}, \quad (5)$$

where $\Delta_{\rm c}$ is the over–density at virialization relative to the critical density. For a WMAP5 cosmology we adopt here the fitting formula $\Delta_{\rm c} = 18\pi^2 + 82d - 39d^2$ (Bryan & Norman 1998), where $d \equiv \Omega_m^z - 1$ is evaluated at the collapse redshift, so that $\Omega_m^z = \Omega_m(1+z)^3/(\Omega_m(1+z)^3 + \Omega_\Lambda + \Omega_k(1+z)^2)$. It is well known that the major merger rate is an increasing function of halo mass or circular velocity. In fact we find that the expected number of mergers between $z = 0$ and $z = 3$ with mass ratio $\xi > 0.3$ is $\simeq 0.4$ for $M_h = 10^8 M_{\odot}$, $\simeq 0.5$ for $M_h = 10^9 M_{\odot}$, $\simeq 0.7$ for $M_h = 10^{10} M_{\odot}$, $\simeq 1.0$ for $M_h = 10^{11} M_{\odot}$, $\simeq 1.4$ for $M_h = 10^{12} M_{\odot}$, $\simeq 1.8$ for $M_h = 10^{13} M_{\odot}$.

In order to calculate the luminosity function of active black holes and to follow the black hole mass growth during each accretion event, we also need to calculate the mass inflow rate. This is assumed to scale with the Eddington rate for the MBH, and is based on the results of merger simulations, which heuristically track accretion onto a central MBH (Di Matteo, Springel & Hernquist 2005; Hopkins et al. 2005; Sijacki et al. 2007). The time spent by a given simulated AGN at a given bolometric luminosity[1] per logarithmic interval is approximated by Hopkins et al. (2005) as:

$$\frac{dt}{dL} = |\alpha| t_Q\, L^{-1}\left(\frac{L}{10^9 L_{\odot}}\right)^{\alpha}, \quad (6)$$

where $t_Q \simeq 10^9$ yr, and $\alpha = -0.95 + 0.32\log(L_{\rm peak}/10^{12}L_{\odot})$. Here $L_{\rm peak}$ is the luminosity of the AGN at the peak of its activity. Hopkins et al. (2006) show that approximating $L_{\rm peak}$ by the Eddington luminosity of the MBH at its final mass (i.e., when it sits on the $M_{\rm BH} - \sigma_c$ relation) compared to computing the peak luminosity with equation (6) above gives the same result and in fact, the difference between these two cases is negligible. Volonteri, Salvaterra & Haardt (2006) derive the following simple differential equation to express the instantaneous accretion

[1]We convert accretion rate into luminosity assuming that the radiative efficiency equals the binding energy per unit mass of a particle in the last stable circular orbit. We associate the location of the last stable circular orbit with the spin of the MBHs, by self-consistently tracking the evolution of black hole spins throughout our calculations (Volonteri 2006). We set 20% as the maximum value of the radiative efficiency, corresponding to a spin slightly below the theoretical limit for thin disc accretion (Thorne 1974).

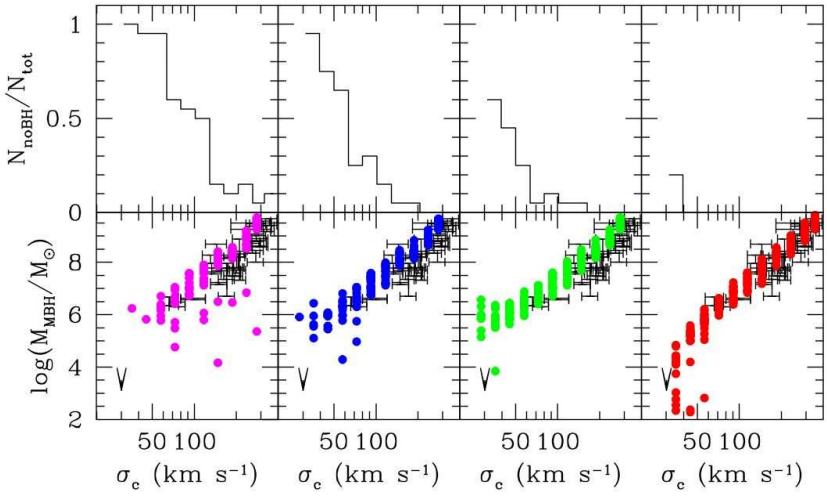

Figure 3. The $M_{\rm bh}-$velocity dispersion (σ_c) relation at $z = 0$. Every circle represents the central MBH in a halo of given σ_c. Observational data are marked by their quoted errorbars, both in σ_c, and in $M_{\rm bh}$ (Tremaine et al. 2002). Left to right panels: $Q_{\rm c} = 1.5$, $Q_{\rm c} = 2$, $Q_{\rm c} = 3$, Population III star seeds. *Top panels:* fraction of galaxies at a given velocity dispersion which **do not** host a central MBH.

rate ($f_{\rm Edd}$,in units of the Eddington rate) for a MBH of mass $M_{\rm BH}$ in a galaxy with velocity dispersion σ_c:

$$\frac{df_{\rm Edd}(t)}{dt} = \frac{f_{\rm Edd}^{1-\alpha}(t)}{|\alpha| t_Q} \left(\frac{\epsilon \dot{M}_{\rm Edd} c^2}{10^9 L_\odot} \right)^{-\alpha}, \tag{7}$$

where here t is the time elapsed from the beginning of the accretion event. Solving this equation provides us with the instantaneous Eddington ratio for a given MBH at a specific time, and therefore we can self-consistently follow the MBH mass. We set the Eddington ratio $f_{\rm Edd} = 10^{-3}$ at $t = 0$. This same type of accretion is assumed to occur, at $z > 15$, following a major merger in which a MBH is not fed by disc instabilities.

4. Results

The repercussions of different initial efficiencies for seed formation for the overall evolution of the MBH population stretch from high-redshift to the local Universe. Detection of gravitational waves from seeds merging at the redshift of formation (Sesana 2007) is probably one of the best ways to discriminate among formation mechanisms. On the other hand, the imprint of different formation scenarios can also be sought in observations at lower redshifts. The various seed formation scenarios have distinct consequences for the properties of the MBH population at $z = 0$.

4.1 Low redshift predictions

4.1.1 *Supermassive black holes in dwarf galaxies*

Obviously, a higher density of MBH seeds implies a more numerous population of MBHs at later times, which can produce observational signatures in statistical samples. More subtly, the formation of seeds in a ΛCDM scenario follows the cosmological bias. As a consequence, the progenitors of massive galaxies (or clusters of galaxies) have a higher probability of hosting MBH seeds (cf. Madau & Rees 2001). In the case of low-bias systems, such as isolated dwarf galaxies, very few of the high-z progenitors have the deep potential wells needed for gas retention and cooling, a prerequisite for MBH formation. In the lowest efficiency model A, for example, a galaxy needs of order 25 massive progenitors (mass above $\sim 10^7 M_\odot$) to ensure a high probability of seeding within the merger tree. In model C, instead, the requirement drops to 4 massive progenitors, increasing the probability of MBH formation in lower bias halos.

The signature of the efficiency of the formation of MBH seeds will consequently be stronger in isolated dwarf galaxies. Figure 3 (bottom panel) shows a comparison between the observed $M_{\rm BH} - \sigma$ relation and the one predicted by our models (shown with circles), and in particular, from left to right, the three models based on the LN06 and Lodato & Natarajan (2007) seed masses with $Q_{\rm c} = 1.5$, 2 and 3, and a fourth model based on lower-mass Population III star seeds. The upper panel of Figure 3 shows the fraction of galaxies that **do not** host any massive black holes for different velocity dispersion bins. This shows that the fraction of galaxies without a MBH increases with decreasing halo masses at $z = 0$. A larger fraction of low mass halos are devoid of central black holes for lower seed formation efficiencies. Note that this is one of the key discriminants between our models and those seeded with Population III remnants. As shown in Figure 3, there are practically no galaxies without central BHs for the Population III seeds.

We can therefore make quantitative predictions for the local occupation fraction of MBHs. Our model A predicts that below $\sigma_c \approx 60\,{\rm kms}^{-1}$ the probability of a galaxy hosting a MBH is negligible. With increasing MBH formation efficiencies, the minimum mass for a galaxy that hosts a MBH decreases, and it drops below our simulation limits for model C. On the other hand, models based on lower mass Population III star remnant seeds, predict that massive black holes might be present even in low mass galaxies. Our predictions have been corroborated by recent observations of low mass galaxies (Kormendy & Bender 2011).

Although there are degeneracies in our modeling (e.g., between the minimum redshift for BH formation and the instability criterion), the BH occupation fraction and the masses of the BHs in dwarf galaxies are the key diagnostics. An additional caveat worth mentioning is the possibility that a galaxy is devoid of a central MBH because of dynamical ejections (due to either the gravitational recoil or three-body scattering). The signatures of such dynamical interactions should be more prominent in dwarf galaxies, but ejected MBHs would leave observational signatures on their hosts (Gültekin et al. in prep.). On top of that, Schnittman (2007) and Volonteri, Lodato & Natarajan (2008) agree in considering the recoil a minor correction to the overall distribution of the MBH population at low redshift (cf. figure 4 in Volonteri 2007).

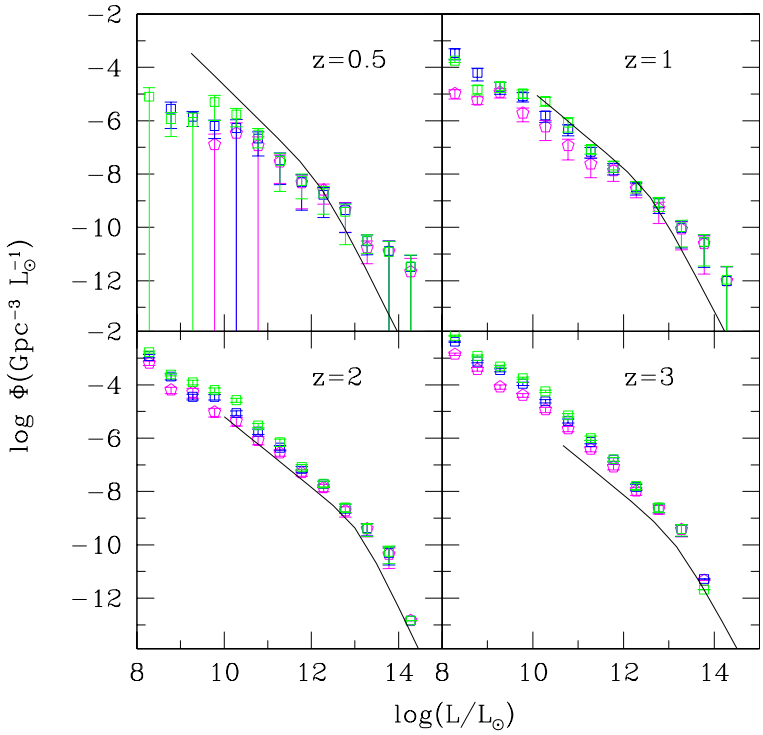

Figure 4. Predicted bolometric luminosity functions at different redshifts with observational data overplotted. All 3 models match the observed bright end of the LF at high redshifts and predict a steep slope at the faint end down to $z = 1$. The 3 models are not really distinguishable with the LF. However at low redshifts, for instance at $z = 0.5$, all 3 models are significantly flatter at both high and low luminosities and do not adequately match the current data. As discussed in the text, the LF is strongly determined by the accretion prescription, and what we see here is simply a reflection of that fact.

Additionally, as MBH seed formation requires halos with low angular momentum (small spin parameter), we envisage that low surface brightness, bulge-less galaxies with large spin parameters (i.e. large discs) are systems where MBH seed formation is less probable. Furthermore, bulgeless galaxies are believed to have preferentially quieter merger histories and are unlikely to have experienced major mergers that could have brought in a MBH from a companion galaxy.

4.1.2 *Comoving mass density of black holes*

Since during the quasar epoch MBHs increase their mass by a large factor, signatures of the seed formation mechanisms are likely more evident at *earlier epochs*. We compare in Figure 5 the integrated comoving mass density in MBHs to the expectations from Sołtan-type arguments, assuming that quasars are powered by radiatively efficient flows (for details, see Yu & Tremaine

2002; Elvis, Risaliti & Zamorini 2002; Marconi et al. 2004). While during and after the quasar epoch the mass densities in models A, B, and C differ by less than a factor of 2, at $z > 3$ the differences are more pronounced.

A very efficient seed MBH formation scenario can lead to a very large BH density at high redshifts. For instance, in the highest efficiency model C with $Q_c = 3$, the integrated MBH density at $z = 10$ is already $\sim 25\%$ of the density at $z = 0$. The plateau at $z > 6$ is due to our choice of scaling the accreted mass with the $z = 0$ $M_{bh} - \sigma$ relation. Since in our models we let MBHs accrete mass that scales with the fifth power of the circular velocity of the halo, the accreted mass is a small fraction of the MBH mass (see the discussion in (Marulli et al. 2006), and the overall growth remains small, as long as the mass of the seed is larger than the accreted mass, which, for our assumed scaling, happens whenever the mass of the halo is below a few times $10^{10} M_{\odot}$. The comoving mass density, an integral constraint, is reasonably well determined out to $z = 3$ but is poorly known at higher redshifts. All models appear to be satisfactory and consistent with current observational limits (shown as the shaded area).

4.1.3 *Black hole mass function at $z = 0$*

One of the key diagnostics is the comparison of the measured and predicted BH mass function at $z = 0$ for our 3 models. In Figure 6, we show (from left to right, respectively) the mass function predicted by models A, B, C and Population III remnant seeds compared to that obtained from measurements. The histograms show the mass function obtained with our models (where the upper histogram includes all the black holes while the lower one only includes black holes found in central galaxies of halos in the merger-tree approach). The two lines are two different estimates of the observed black hole mass function. In the upper one, the measured velocity dispersion function for nearby late and early-type galaxies from the SDSS survey (Bernardi et al. 2003; Sheth et al. 2003) has been convolved with the measured $M_{BH} - \sigma$ relation. We note here that the scatter in the $M_{bh} - \sigma$ relation is not explicitly included in this treatment, however the inclusion of the scatter is likely to preferentially affect the high mass end of the BHMF, which provides stronger constraints on the accretion histories than do the seed masses. It has been argued by Tundo et al. (2007), Bernardi et al. (2007) and Lauer et al. (2007) that the BH mass function differs if the bulge mass is used instead of the velocity dispersion in relating the BH mass to the host galaxy. Since our models do not trace the formation and growth of stellar bulges in detail, we are restricted to using the velocity dispersion in our analysis.

The lower dashed curve is an alternate theoretical estimate of the BH mass function derived using the Press-Schechter formalism from Jenkins et al. (2001) in conjunction with the observed $M_{BH} - \sigma$ relation. Selecting only the central galaxies of halos in the merger-tree approach adopted here (lower histograms) is shown to be equivalent to this analytical estimate, and this is clearly borne out in the plot. When we include black holes in satellite galaxies (upper histograms, cf. the discussion in Volonteri, Haardt & Madau 2003) the predicted mass function moves towards the estimate based on SDSS galaxies. The higher efficiency models clearly produce more BHs. At higher redshifts, for instance at $z = 6$, the mass functions of active MBHs predicted by all models

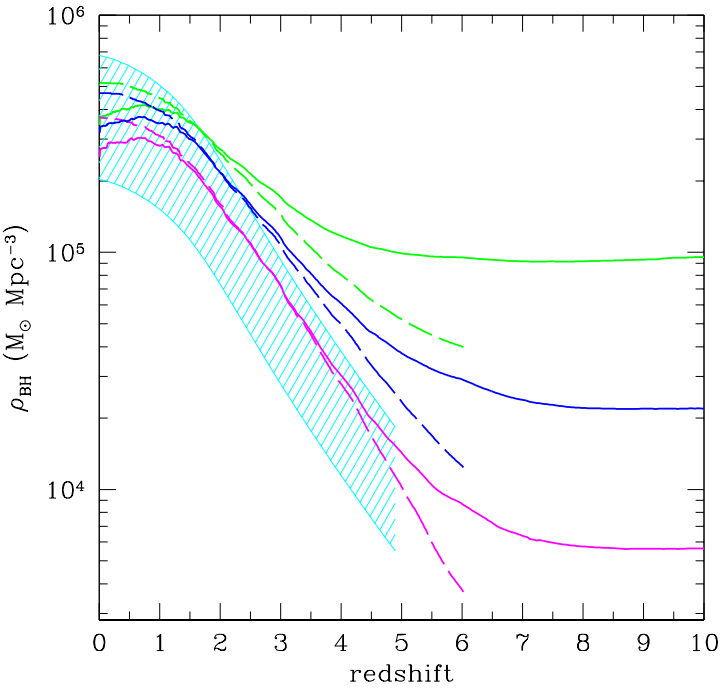

Figure 5. Integrated black hole mass density as a function of redshift. Solid lines: total mass density locked into nuclear black holes. Dashed lines: integrated mass density accreted by black holes. Models based on BH remnants of Population III stars (lowest curve), $Q_{\rm c} = 1.5$ (middle curve) and $Q_{\rm c} = 2$ (upper curve). Shaded area: constraints from Sołtan-type arguments, where we have varied the radiative efficiency from a lower limit of 6% (applicable to Schwarzschild MBHs, upper envelope of the shaded area), to about 20%. All 3 massive seed formation models are in comfortable agreement with the mass density obtained from integrating the optical luminosity functions of quasars.

are in very good agreement, in particular for BH masses larger than $10^6\,M_\odot$, as it is the growth by accretion that dominates the evolution of the population. At the highest mass end ($> 10^9\,M_\odot$) model A lags behind models B and C, although we stress once again that our assumptions for the accretion process are very conservative.

The *relative* differences between models A, B, and C at the low-mass end of the mass function, however, are genuinely related to the MBH seeding mechanism (see also Figures 3 and 5). In model A, simply, fewer galaxies host a MBH, hence reducing the overall number density of black holes. Although our simplified treatment does not allow robust quantitative predictions, the presence of a "bump" at $z = 0$ in the MBH mass function at the characteristic mass that marks the peak of the seed mass function (cf. Figure 2) is a sign of highly efficient formation of massive seeds (i.e., much larger mass than, for instance, Population III remnants). The higher the efficiency of seed formation, the more pronounced is the bump (note that the bump is most prominent for model C). Since current measurements of MBH masses extend barely down to $M_{\rm bh} \sim 10^6 M_\odot$,

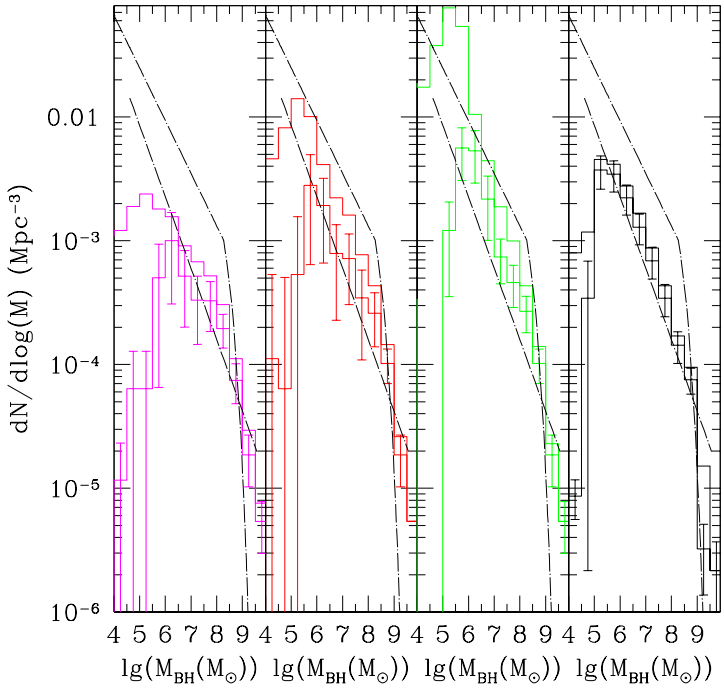

Figure 6. Mass function of black holes at z=0. Histograms represent the results of our models, including central galaxies only (lower histograms with error bars), or including satellites in groups and clusters (upper histograms). Left panel: $Q_c = 1.5$, mid-left panel: $Q_c = 2$, mid-right panel: $Q_c = 3$, right panel: models based on BH remnants of Population III stars. Upper dashed line: mass function derived from combining the velocity dispersion function of Sloan galaxies (Sheth et al. 2003, where we have included the late-type galaxies extrapolation), and BH mass-velocity dispersion correlation (e.g., Tremaine et al. 2002). Lower dashed line: mass function derived using the Press-Schechter formalism from Jenkins et al. (2001) in conjunction with the $M_{BH} - \sigma$ relation (Ferrarese 2002).

this feature cannot be observationally tested with present data, but future campaigns, with the Giant Magellan Telescope or JWST, are likely to extend the mass function measurements to much lower black hole masses.

4.2 Predictions at high redshift

4.2.1 *The luminosity function of accreting black holes*

Turning to the global properties of the MBH population, as suggested by Yu & Tremaine (2002), the mass growth of the MBH population at $z < 3$ is dominated by the mass accreted during the bright epoch of quasars, thus washing out most of the imprint of initial conditions. This is

evident when we compute the luminosity function of AGN. Clearly the detailed shape of the predicted luminosity function depends most strongly on the accretion prescription used. With our assumption that the gas mass accreted during each merger episode is proportional to V_c^5, we find that distinguishing between the various seed models is difficult. As shown in Figure 4, all 3 models reproduce the bright end of the observed bolometric LF (Hopkins, Richards & Hernquist 2007) at higher redshifts (marked as the solid curve in all the panels), and predict a fairly steep faint end that is as yet undetected. All models fare less well at low redshift, shown in particular at $z = 0.5$. This could be due to the fact that we have used a single accretion prescription to model growth at all times. On the other hand, the decline in the available gas supply at low redshifts (since the bulk of the gas has been consumed before this epoch by star formation activity) likely changes the radiative efficiency of these systems. Besides, observations suggest a sharp decline in the number of actively accreting black holes at low redshifts at different wave-lengths, produced most probably by changes in the accretion flow as a result of changes in the geometry of the nuclear regions of galaxies. In fact, all 3 of our models under-predict the slope at the faint end. There are three other effects that could cause this flattening of the LF at the faint end at low redshift for our models: (i) not having taken into account the result of on-going mergers and the fate of satellite galaxies; (ii) the number of realizations generated and tracked is insufficient for statistics, as evidenced by the systematically larger errorbars and (iii) more importantly, it is unclear if merger-driven accretion is indeed the trigger of BH fueling in the low redshift Universe. We note that the 3 massive seed models and Population III seed model cannot be discriminated by the LF at high redshifts. Models B and C are also in agreement viz-a-viz the predicted BH mass function at $z = 6$ (see Figure 2), even assuming a very high radiative efficiency (up to 20%), while model A might need less severe assumptions, in particular for BH masses larger than $10^7\ M_\odot$.

5. Conclusions

Ih this review, we outline massive black hole seed formation models and focus on the predictions made by these at high and low redshift. While the errors on mass determinations of local black holes are large at the present time, definite trends with host galaxy properties are observed. The tightest correlation appears to be between the BH mass and the velocity dispersion of the host spheroid. Starting with the ab-initio black hole seed mass function computed in the context of direct formation of central objects from the collapse of pre-galactic discs in high redshift halos, we follow the assembly history to late times using a Monte Carlo merger tree approach. Key to our calculation of the evolution and build-up of mass is the prescription that we adopt for determining the precise mass gain during a merger. Motivated by the phenomenological observation of $M_{\rm BH} \propto V_{\rm c}^5$, we assume that this proportionality carries over to the gas mass accreted in each step. With these prescriptions, a range of predictions can be made for the mass function of black holes at high and low z, and for the integrated mass density of black holes, all of which are observationally determined. We evolve 3 models, designated model A, B and C, which correspond to increasing efficiencies respectively for the formation of seeds at high redshift. These models are compared to one in which the seeds are remnants of Population III stars.

It is important to note here that one major uncertainty prevents us from making more concrete

predictions: the unknown metal enrichment history of the Universe. Key to the implementation of our models is the choice of redshift at which massive seed formation is quenched. The direct seed formation channel described here ceases to operate once the Universe has been enriched by metals that have been synthesized by the first generation of stars. Once metals are available in the Inter-Galactic Medium, gas cooling is much more efficient and hydrogen in either atomic or molecular form is no longer the key player. In this work, we have assumed this transition redshift to be $z = 15$. The efficiency of MBH formation and the transition redshift are somehow degenerate (e.g., a model with $Q = 1.5$ and enrichment redshift $z = 12$ is halfway between model A and model B); if other constraints on this redshift were available we could considerably tighten our predictions.

Below we list our predictions and compare how they fare with respect to current observations. The models investigated here clearly differ in predictions at the low mass end of the black hole mass function. With future observational sensitivity in this domain, these models can be distinguished.

1. Occupation fraction at $z = 0$: Our model for the formation of relatively high-mass black hole seeds in high-z halos has direct influence on the black hole occupation fraction in galaxies at $z = 0$. All our models predict that low surface brightness, bulge-less galaxies with large spin parameters (i.e. large discs) are systems where MBH formation is least probable. We find that a significant fraction of low-mass galaxies might not host a nuclear black hole. This is in very good agreement with the shape of the $M_{\rm bh}-\sigma$ relation determined recently from an observational census (an HST ACS survey) of low mass galaxies in the Virgo cluster reported by Ferrarese et al. (2006). While current data in the low mass regime are scant (Barth 2004; Greene & Ho 2007; Kormendy & Bender 2011), future instruments and surveys are likely to probe this region of parameter space with significantly higher sensitivity.

2. High mass end of the local SMBH mass function: While the models studied here (with different black hole seed formation efficiencies) are distinguishable at the low mass end of the BH mass function, at the high mass end the effect of initial seeds appears to be less important. These models cannot be easily distinguished by observations at $z \sim 3$.

One of the key caveats of our picture is that it is unclear whether the differences produced by different seed models on observables at $z = 0$ might be compensated or masked by BH fueling modes at earlier epochs. There could be other channels for BH growth that dominate at low redshifts like minor mergers, dynamical instabilities, accretion of molecular clouds and tidal disruption of stars. The decreased importance of the merger driven scenario is patent from observations of low-redshift AGN, which are for the large majority hosted by undisturbed galaxies (e.g. Pierce et al. 2007 and references therein) in low-density environments. However, the feasibility and efficiency of some alternative channels are still to be proven, for example, the efficiency of feeding from large scale instabilities (see discussion in King & Pringle 2007; Shlosman, Frank & Begelman 1989; Goodman 2003; Collin 1999). In any event, while these additional channels

for BH *growth* can modify the detailed shape of the mass function of MBHs, or of the luminosity function of quasars, they will not create new MBHs. The occupation fraction of MBHs (see Figure 3) is therefore largely *independent* of the accretion mechanism and a true signature of the formation process.

To date, most theoretical models for the evolution of MBHs in galaxies do not include *how* MBHs form. This work is a first analysis of the observational signatures of massive black hole formation mechanisms in the low redshift Universe, complementary to the investigation by Sesana, Volonteri & Haardt (2007), where the focus was on detection of seeds at the very early times when they form, via gravitational waves emitted during MBH mergers. We focus here on possible dynamical signatures that forming massive black hole seeds carry over to the local Universe. Obviously, the signatures of seed formation mechanisms will be far more clear if considered jointly with the evolution of the spheroids that they host. The mass, and especially the frequency, of the forming MBH seeds is a necessary input when investigating how the feedback from accretion onto MBHs influences the host galaxy, and is generally introduced in numerical models using extremely simplified, *ad hoc* prescriptions (e.g., Springel, Di Matteo & Hernquist 2005; Di Matteo, Springel & Hernquist 2005; Hopkins et al. 2006; Croton et al. 2005; Cattaneo et al 2006; Bower et al. 2006). Adopting more detailed models for black hole seed formation, as outlined here, can in principle strongly affect such results. Incorporating sensible assumptions for the masses and frequency of MBH seeds in models of galaxy formation is necessary if we want to understand the symbiotic growth of MBHs and their hosts.

Acknowledgements

PN would like to acknowledge her collaborators Marta Volonteri and Giuseppe Lodato with whom most of this work was done. She would also like to thank the John Simon Guggenheim Foundation for support from a Guggenheim fellowship and the Institute for Theory and Computation at Harvard University for hosting her.

References

Barth A.J., 2004, IAU Symp., 222, 3
Begelman M.C., Volonteri M., Rees M.J., 2006, MNRAS, 370, 289
Bernardi M., et al., 2003, AJ, 125, 1817
Bernardi M., Sheth R.K., Tundo E., Hyde J.B., 2007, ApJ, 660, 267
Bower R., et al., 2006, MNRAS, 370, 645
Bryan G., Norman M., 1998, ApJ, 495, 80
Cattaneo A., Dekel A., Devriendt J., Guiderdoni B., Blaizot J., 2006, MNRAS, 370, 1651
Collin S., 1999, Phys Rep., 311, 463
Croton D., et al., 2005, MNRAS, 356, 1155
Di Matteo T., Springel V., Hernquist L., 2005, Nature, 433, 604
D'Onghia E., Navarro J., 2007, MNRAS, 380, L58
Elvis M., Risaliti G., Zamorani G., 2002, ApJ, 565, L75
Fabian A.C., 2002, ASPC, 258, 185

Fakhouri O., Ma C.-P., Boylan-Kolchin M., 2010, MNRAS, 406, 2267
Fan X., et al., 2004, AJ, 128, 515
Fan X., et al., 2006, AJ, 132, 117
Ferrarese L., 2002, ApJ, 572, 90
Ferrarese L., Merritt D., 2000, ApJ, 539, L9
Ferrarese L., et al., 2006, ApJS, 164, 334
Gebhardt K., et al., 2003, ApJ, 583, 92
Goodman J., 2003, MNRAS, 337, 937
Greene J., Ho, L., 2007, ApJ, 670, 92
Gültekin K., et al., 2009, ApJ, 698, 198
Haehnelt M., Natarajan P., Rees M. J., 1998, MNRAS, 300, 817
Haiman Z., Loeb A., 1998, ApJ, 503, 505
Häring N., Rix H.-W., 2004, ApJ, 604, L89
Hopkins P.F., Hernquist L., Cox T.J., Di Matteo T., Robertson B., Springel V., 2005, ApJ, 630, 716
Hopkins P.F., Hernquist L., Martini P., Cox T.J., Robertson B., Di Matteo T., Springel V., 2005, ApJ, 625, L71
Hopkins P.F., Richards G.T., Hernquist L., 2007, 654, 731
Jenkins A., Frenk C.S., White S.D.M., Colberg J.M., Cole S., Evrard A.E., Couchman H.M.P., Yoshida N., 2001, MNRAS, 321, 372
Kauffmann G., Haehnelt M., 2000, MNRAS, 311, 576
King A., 2003, ApJ, 596, L27
King A.R., Pringle J.E., 2007, MNRAS, 377, L25
Kormendy J., Bender R., 2011, Nature, 469, 377
Koushiappas S.M., Bullock J.S., Dekel A., 2004, MNRAS, 354, 292
Lauer T., Tremaine S., Richstone D., Faber S. M., 2007, 670, 249
Lodato G., Natarajan P., 2006, MNRAS, 371, 1813 (LN06)
Lodato G., Natarajan P., 2007, MNRAS, 377, L64
Madau P., Rees M. J., 2001, ApJ, 551, L27
Marconi A., Hunt L., 2003, ApJ, 598, L21
Marconi A., Risaliti G., GIlli R., Hunt L.K., Maiolino R., Salvati M., 2004, MNRAS, 351, 169
Marulli F., Crociani D., Volonteri M., Branchini E., Moscardini L., 2006, MNRAS, 368, 1269
Natarajan P., Treister E., 2009, MNRAS, 393, 838
Pierce C.M., et al., 2007, ApJ, 660, L19
Schnittmann J., 2007, ApJ, 667, L133
Sesana A., 2007, MNRAS, 382, L6
Sesana A., Volonteri M., Haardt, F., 2007, MNRAS, 377, 1711
Sheth R., et al., 2003, ApJ, 594, 225
Shlosman I., Frank J., Begelman M.C., 1989, Nature, 338, 45
Sijacki D., Springel V., Di Matteo T., Hernquist, L., 2007, MNRAS, 380, 877
Silk J., Rees M. J., 1998, A&A, 331, L1
Springel V., Di Matteo T., Hernquist, L., 2005, ApJ, 620, L79
Thompson T.A., Quataert E., Murray N., 2005, ApJ, 630, 167
Thorne K., 1974, ApJ, 191, 507
Tremaine S., et al., 2002, ApJ, 574, 740
Tundo E., Bernardi M., Hyde J., Sheth R., Pizzella A., 2007, ApJ, 663, 53
Vivitska M., Klypin A., Kravtsov A., Wechsler R., Primack J., Bullock J., 2002, ApJ 581, 799
Volonteri M., 2006, AIPC, 873, 61
Volonteri M., 2007, ApJ, 663, L5

Volonteri M., Begelman M. C., 2010, MNRAS, 409, 1022
Volonteri M., Natarajan P., 2009, MNRAS, 400, 1911
Volonteri M., Rees M.J., 2005, ApJ, 633, 624
Volonteri M., Gültekin K., Dotti M., 2010, MNRAS, 404, 2143
Volonteri M., Haardt F., Madau P., 2003, ApJ, 582, 559
Volonteri M., Lodato G., Natarajan P., 2008, MNRAS, 383, 1079
Volonteri M., Salvaterra R., Haardt F., 2006, MNRAS, 373, 121
Yu Q., Tremaine S., 2002, MNRAS, 335, 965